Flat lenses constructed by graded negative index-based photonic crystals with tuned configurations

2013 Chinese Phys. B 22 104101

(http://iopscience.iop.org/1674-1056/22/10/104101)

Flat lenses constructed by graded negative index-based photonic crystals with tuned configurations*

Jin Lei(晋 蕾)[a], Zhu Qing-Yi(朱清溢)[a], Fu Yong-Qi(付永启)[a]†, and Yu Wei-Xing(鱼卫星)[b]‡

[a] School of Physical Electronics, University of Electronic Science and Technology of China, Chengdu 610054, China
[b] State Key Laboratory of Applied Optics, Changchun Institute of Optics, Fine Mechanics and Physics, Chinese Academy of Sciences, Changchun 130033, China

(Received 20 November 2012; revised manuscript received 6 March 2013)

Flat lenses are designed by means of graded negative refractive index-based photonic crystals (PCs) constructed using air-holes tuned with different shapes. By gradually modifying the filling factor along the transverse direction, we obtain the graded negative index-based lenses for the purpose of focusing an incident plane wave. The finite-difference and time-domain (FDTD) algorithm is adopted for numerical calculation. Our calculation results indicate that these lenses can finely focus incident plane waves. Moreover, for the same size of air-holes, the focusing properties of the lens with rectangular air-holes are better than those with the other shaped air-holes. The graded negative index PCs lenses could possibly enable new applications in optoelectronic systems.

Keywords: photonic crystals, graded negative index, focusing, flat lenses

PACS: 41.20.Jb, 42.25.Bs, 42.70.Qs **DOI:** 10.1088/1674-1056/22/10/104101

1. Introduction

Metamaterials have aroused the great interest of numerous researchers due to their unusual properties.[1] One of these predominant properties is negative refraction, which makes imaging with sub-wavelength resolution possible.[2–5] By virtue of photonic band structures, negative refraction can also be realized by using photonic crystals (PCs) within some frequency regions. This feature has been used to design and fabricate PC-based superlenses before.[6–9] Negative index-based flat lenses made of metamaterials or PCs do not possess a focal length and cannot provide practical imaging. They cannot be used to focus the collimated incident waves generated from an object at a certain distance. However, this point is important in practical applications. To overcome this shortage, graded index-based lenses have been proposed.[10,11]

A flat slab of PCs with a graded negative index in the transverse direction can focus collimation waves.[12] When the PC lenses work in the second photonic band structures, they behave like an equivalent medium with the negative index.[13] Theoretically, the graded index can be achieved by appropriate gradual modifications of the filling factor,[14–18] lattice constant,[19–22] and material parameters.[15] In the past few years, graded PCs have been explored for focusing,[15–19] mirage,[20–22] self-collimation,[15] and superbending[21] of electromagnetic (EM) waves. Most of the graded index PCs that have been reported before are PCs with circlular air-holes. To our knowledge, the relationship between focal property and shape of the air-hole of PCs has not been reported so far. However, the relationship is important for designing PCs. In order to explore the relationship, we study flat lenses constructed by graded negative index-based PCs with tuned configurations in this paper. Firstly, we design hexagonal lattice PCs which present behaviors of negative refraction. By varying the PC parameters, PC lenses with a graded negative index are derived through our design and are used to focus the incident plane wave. Then we change the shapes of air-holes and record the focusing parameters for the purpose of investigating the relationship between air-hole shape and focal property. The graded negative index PCs can be designed to be highly insensitive to wavelength/frequency, enabling the lenses to perform broadband negative index imaging.[18] An approach to the design of a negative index imaging system is provided. It may be useful to design flat lenses with potential new applications in future optoelectronic systems.

2. Numerical calculation setup

In order to realize negative refraction in the visible region of the electromagnetic spectrum, we constructe a two-dimensional (2D) hexagonal lattice PC constituted by a dielectric medium with air-holes. The refractive index of the dielectric medium is set to be 4. Firstly, the lattice constant is empirically set to be 150 nm.[23] Sizes of the air holes in the

*Project supported by the National Natural Science Foundation of China (Grant Nos. 11079014, 61077010, 90923036, and 60977041) and the 100-Talent Program of the Chinese Academy of Sciences.

†Corresponding author. E-mail: yqfu@uestc.edu.cn
‡Corresponding author. E-mail: yuwx@ciomp.ac.cn

transverse direction vary in such a way that the modulus of the size is smallest in the center of the PC and increases toward the edges. The air-hole shapes are tuned using shapes of ellipse, rectangle, and triangle, respectively.

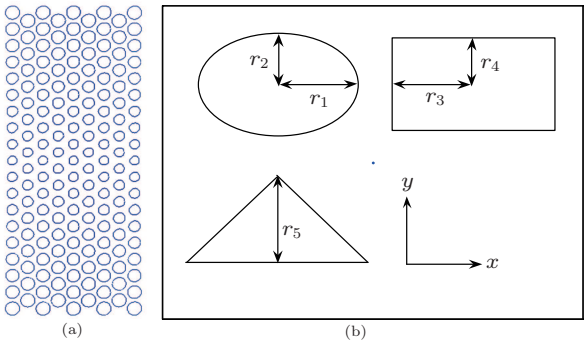

Fig. 1. (color online) (a) Schematic illustration for the graded negative PC lenses with graded air-hole sizes. (b) A schematic illustration for different shape air-holes.

Figure 1(a) shows a schematic illustration for the graded negative PC lenses with graded air-hole sizes. Figure 1(b) shows a schematic illustration for the air-holes with different shapes. The normal of the lenses (x direction) is chosen along the $\Gamma \rightarrow M$ direction, which is the direction of wave propagation. In Fig. 1(b), r_1, r_2, r_3, r_4, and r_5 are the variable parameters of air-holes. We vary the air-hole sizes ranging from 40 nm to 60 nm following the functions of expression (1)

$$\begin{cases} R_1(y) = 0.0148\,|y| + 0.04, \\ R_2(y) = 0.011y^2 + 0.04, \\ R_3(y) = 0.0219\sin(0.85\,|y|) + 0.04. \end{cases} \tag{1}$$

For the same parameters, the area of the triangle hole is small. Therefore, we expand the parameters of triangle hole 1.8 times. There are 12 different types of PCs that we design, and their corresponding numbers are shown in Table 1.

Table 1. Illustration of the numbers of different types of PCs with different parameters.

Number	Types	Number	Types
Ellipse 1	$r_1 = r_2$, both follows function	Rectangle 1	$r_3 = r_4$, both follows function
Ellipse 2	$r_2 = 60$ nm, r_1 follows function	Rectangle 2	$r_4 = 60$ nm, r_3 follows function
Ellipse 3	$r_2 = 40$ nm, r_1 follows function	Rectangle 3	$r_4 = 40$ nm, r_3 follows function
Ellipse 4	$r_1 = 60$ nm, r_2 follows function	Rectangle 4	$r_3 = 60$ nm, r_4 follows function
Ellipse 5	$r_1 = 40$ nm, r_1 follows function	Rectangle 5	$r_3 = 40$ nm, r_4 follows function
Triangle 1	r_5 follows function	Triangle 2	$r_5/1.8$ follows function

We employe a commercial software (FDTD Solution from Lumerical Solution Inc.) to simulate the focusing properties of the PC lenses under plane-wave illumination. The transverse direction of the PC lenses is along the y direction, and the optical axis is along the x direction. The working frequency is $0.25a/\lambda$, and the plane-wave mode is the transverse magnetic (TM) mode.

3. Results and analyses

Figure 2 shows the two-dimensional (2D) distributions of the focus simulated for all types of PCs. It can be seen that all types of the PCs we designed can focus the incident plane wave. The depth of focus of the PCs with ellipse air-holes is longer than that of other types. The PCs with rectangle air-holes possess a high transmittance, and the focal effect of the PCs with triangle air-holes is worst in comparison with the other types of air-holes. In order to facilitate the comparison, we introduce three focusing parameters: amplitude, focused beam spot size, and focal length as shown in Fig. 3. The amplitude is the value of maximum field intensity distributed along the optical axis. The focal length is measured in terms of the location where field intensity along the optical axis is maximum. The spot size is derived at the sites of full-width and half-maximum (FWHM).

Figures 4(a) and 4(b) show the relations among amplitude, focused beam spot size, and focal length. With the increase of focal length, the amplitude decreases and the spot size increases subsequently as shown in Figs. 4(a) and 4(b), respectively. That phenomenon complies with the general optical imaging law. From the practical application point of view, we need the focusing region which has a large amplitude and small spot size. Although the focal length of the PCs with rectangle air-holes is short, it possesses large amplitude and small spot size so that some of the spot sizes can break through diffraction limit. It can be seen from Fig. 4(c) that the intensity profile may have a weak sidelobe in its focal region. The focal parameters of the PC lenses have excellent focal properties, as shown in Table 2. The focal lengths of the PCs lenses with rectangular air-holes are shorter than those with other type air-holes. And the focusing properties of the lenses are also better than those of other lenses.

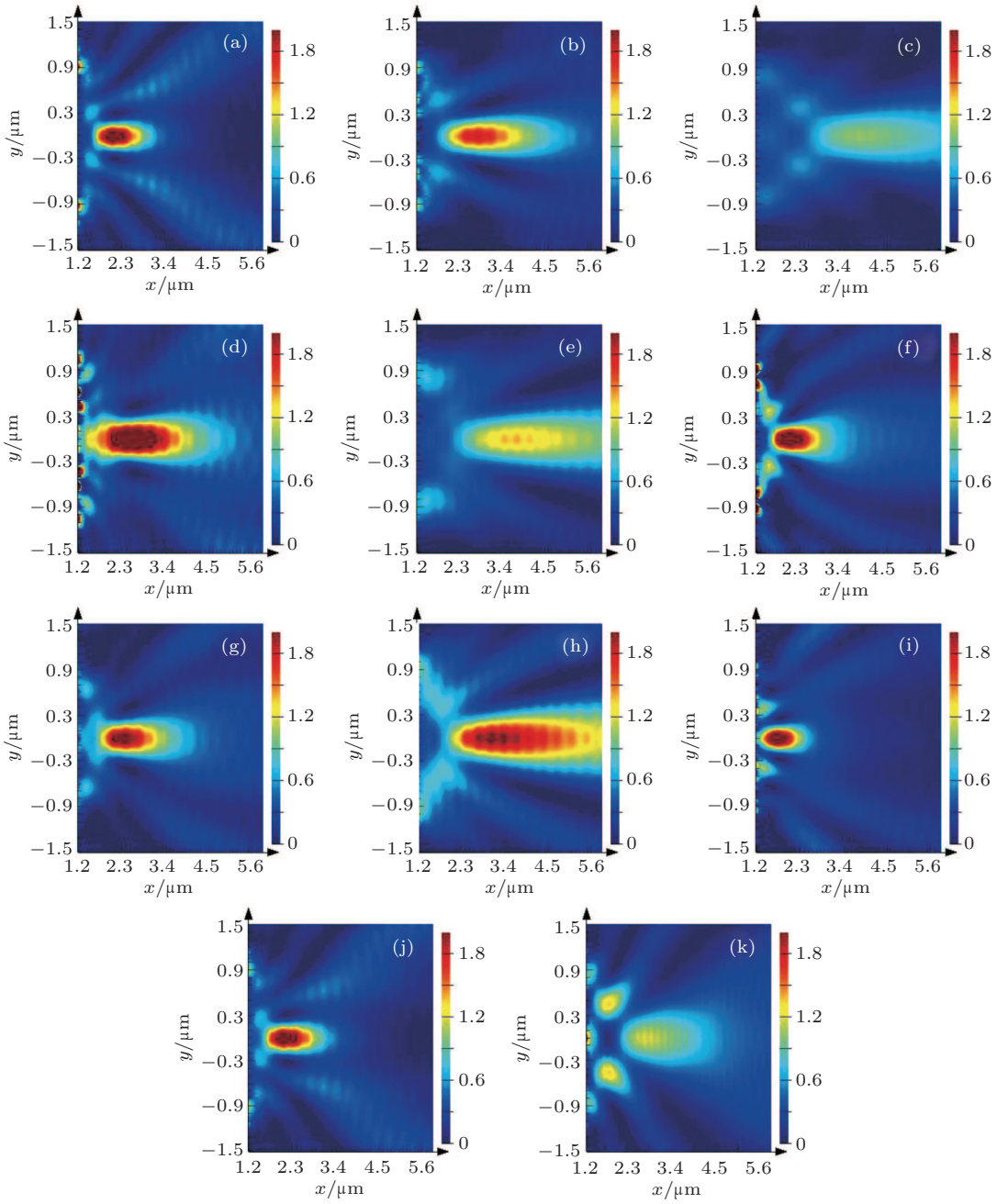

Fig. 2. (color online) Simulated electric intensity distributions behind the PC. The corresponding numbers are (a) ellipse 1, (b) ellipse 2, (c) ellipse 3, (d) ellipse 4, (e) ellipse 5, (f) rectangle 1, (g) rectangle 2, (h) rectangle 3, (i) rectangle 4, (j) rectangle 5, and (k) triangle 2.

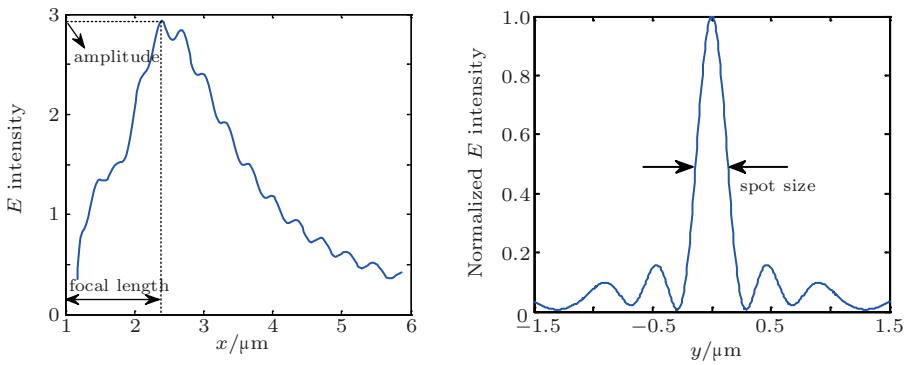

Fig. 3. (color online) Schematic illustrations of focusing parameters.

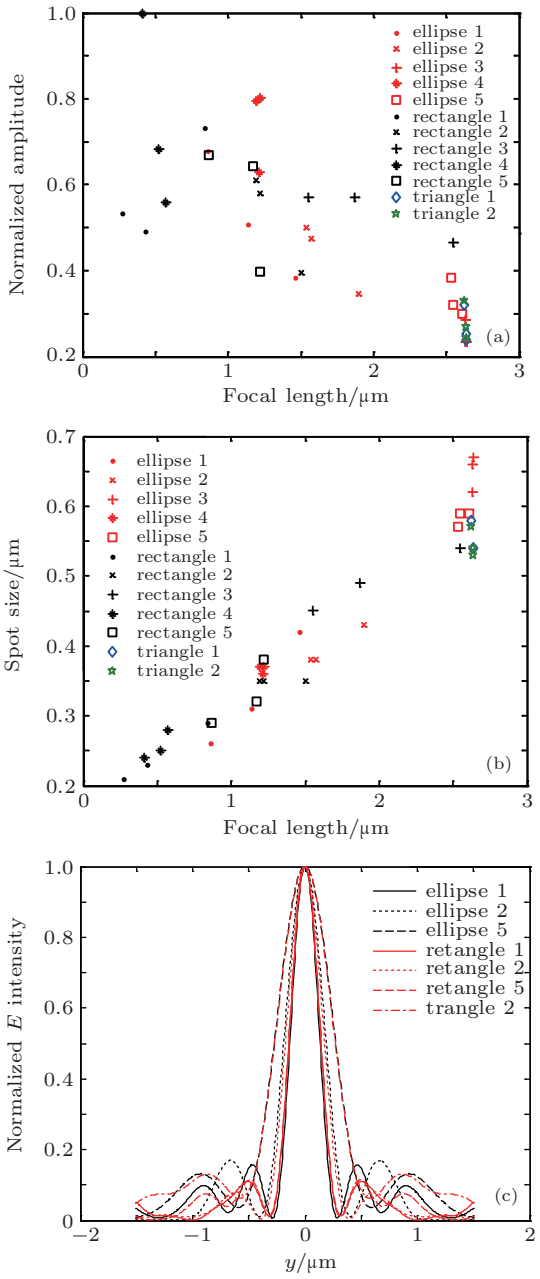

Fig. 4. (color online) (a) Focal lengths and amplitudes with different air-hole shapes. (b) Focal lengths and spot sizes with different air-hole shapes. (c) Intensity distributions along the transverse direction in the focus.

Table 2. Focal parameters of the PCs lenses.

Items	Function	Focal length/μm	Spot size/μm	Amplitude/a.u.
1. $r_1 = r_2$,	R_1	1.14	0.31	1.85
both follow	R_2	1.46	0.42	1.4
function	R_3	0.86	0.26	2.48
2. $r_1 = 60$ nm,	R_1	1.22	0.37	2.93
r_2 follows	R_2	1.19	0.37	2.9
function	R_3	1.21	0.36	2.3
3. $r_3 = r_4$,	R_1	0.41	0.24	4.08
both follow	R_2	0.84	0.31	1.93
function	R_3	0.27	0.26	1.93
4. $r_3 = 60$ nm,	R_1	0.52	0.25	2.49
r_4 follows	R_2	0.57	0.28	2.04
function	R_3	0.41	0.24	3.65

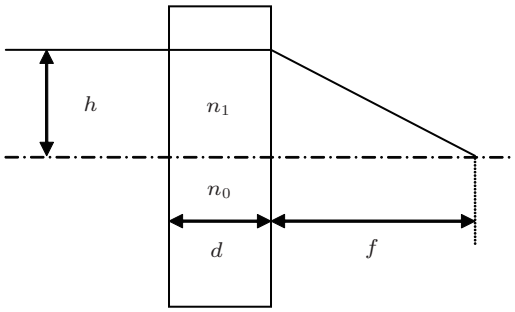

Fig. 5. Schematic diagram for two collimated waves travelling through a flat PC lens.

We consider two waves which travel across the graded PC lenses in the center and on the edge then converge at a focal length f behind the lens as shown in Fig. 5. According to Fermat's principle, we deduce Eqs. (2) and (3) as shown in the following

$$n_0 d + f = n_1 d + \sqrt{h^2 + f^2}, \tag{2}$$

$$f = \frac{h^2}{2d}\frac{1}{n_0 - n_1} - \frac{d}{2}(n_0 - n_1). \tag{3}$$

With Eq. (3), we can derive the value of $(n_0 - n_1)$ required for the desired f and the focal length that decreases with the value of $(n_0 - n_1)$ increasing.

An FDTD solution is employed here to calculate the photonic band structures of the designed hexagonal lattice PCs working in the TM mode, and the first three photonic bands are shown in Figs. 6(a)–6(d). For the working frequency $0.25a/\lambda$, the PC lenses with different parameters have different values of wave vector $\boldsymbol{k}$ and work in the second photonic band. By the definition of the group velocity $\boldsymbol{v}_g = \nabla_k(\omega(\boldsymbol{k}))$, $\boldsymbol{v}_g$ is always oriented in the direction perpendicular to the equifrequency surface (EFS) in the direction along the increase of $\omega(\boldsymbol{k})$. Each PC lens behaves like an equivalent medium with the negative index at the working frequency.[24] Each PC lens can be characterized by an effective refractive index $n = -|\boldsymbol{k}|c/\omega$. The d-values of effective refractive index are determined in the following equation:

$$\begin{cases} \Delta n_1 = n_{r_1=r_2=0.06\ \mu\text{m}} - n_{r_1=r_2=0.04\ \mu\text{m}}, \\ \Delta n_2 = n_{r_1=r_2=0.06\ \mu\text{m}} - n_{r_1=0.04\ \mu\text{m}, r_2=0.06\ \mu\text{m}}, \\ \Delta n_3 = n_{r_3=r_4=0.06\ \mu\text{m}} - n_{r_3=r_4=0.04\ \mu\text{m}}, \\ \Delta n_4 = n_{r_3=r_4=0.06\ \mu\text{m}} - n_{r_3=0.04\ \mu\text{m}, r_4=0.06\ \mu\text{m}}, \\ \Delta n_5 = n_{r_5=0.06\ \mu\text{m}} - n_{r_5=0.04\ \mu\text{m}}, \\ \Delta n_6 = n_{r_5=0.084\ \mu\text{m}} - n_{r_5=0.056\ \mu\text{m}}. \end{cases} \tag{4}$$

It can be seen from Fig. 6 that they obey the relation of

$$\Delta n_3 > \Delta n_4 > \Delta n_1 > \Delta n_2 > \Delta n_6 > \Delta n_5.$$

With Eq. (3), the focal lengths are in accordance with the law that $f_3 < f_4 < f_1 < f_2 < f_6 < f_5$. It complies with the calculation results.

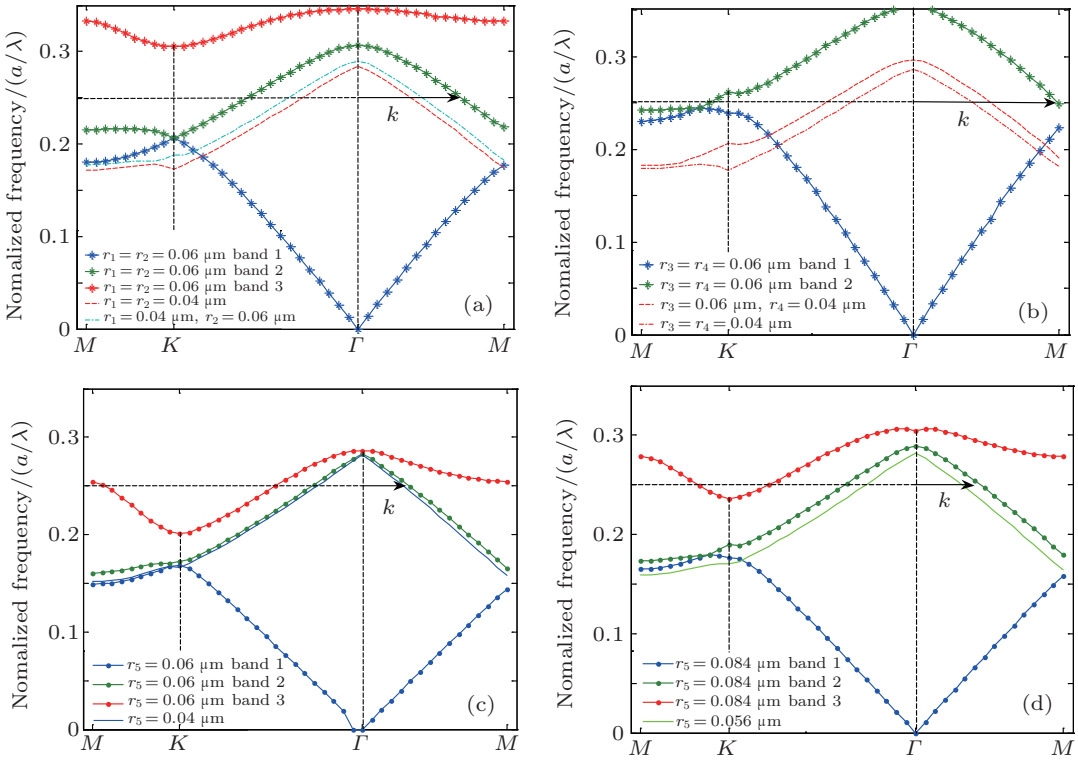

Fig. 6. (color online) Calculated band structures of the designed hexagonal lattice PC lenses with different types of tuned configurations of (a) circular air-holes, (b) rectangular air-holes, and (c) triangle air-holes. (d) Band structure of the designed hexagonal lattice PC lens with triangle air-holes and the air-hole size is expanded 1.8 times.

4. Conclusion

In this paper, we designed hexagonal lattice PC lenses which can present negative refraction behavior. By varying the lens parameters and changing the shape of the air-hole, PC lenses with a graded negative index are obtained and used for focusing the plane wave. Then we use the finite-difference and time-domain (FDTD) algorithm for numerical calculation. By analyzing the calculation results, we find that the focusing parameters comply with the general optical imaging law and the lenses with rectangular air-holes can generate good focusing properties. Our calculated band structures demonstrate that the variation rule of the focal length is consistent with that of the previous theoretical results.

References

[1] Smith D R, Pendry J B and Wiltshire M C K 2004 *Science* **305** 788
[2] Shelby R A, Smith D R and Schultz S 2001 *Science* **292** 77
[3] Pendry J B 2000 *Phys. Rev. Lett.* **85** 3966
[4] Fang N, Lee H, Sun C and Zhang X 2005 *Science* **308** 534
[5] Li C and Li F 2005 *Chin. Phys. Lett.* **23** 470
[6] Luo C Y, Johnson S G, Joannopoulos J D and Pendry J B 2002 *Phys. Rev. B* **65** 201104
[7] Parimi P V, Lu W T, Vodo P and Sridhar S 2003 *Nature* **426** 404
[8] Schonbrun E, Yamashita T, Park W and Summers C J 2006 *Phys. Rev. B* **73** 195117
[9] Schonbrun E, Wu Q, Park W, Yamashita T, Summers C J, Abashin M and Fainman Y 2007 *Appl. Phys. Lett.* **90** 041113
[10] Parazzoli C G, Greegor R B, Nielsen J A, Thompson M A, Li K, Vetter A M and Tanielian M H 2004 *Appl. Phys. Lett.* **84** 3232
[11] Casse B D F, Lu W T, Huang Y J and Sridhar S 2008 *Appl. Phys. Lett.* **93** 053111
[12] Gomwz-Reino C, Perez M V and Bao C 2002 *Gradient-Index Optics: Fundamentals and Applications* (Berlin: Springer) p. 127
[13] Berrier A, Mulot M, Swillo M, Qiu M, Thyleń L, Talneau A and Anand S 2004 *Phys. Rev. Lett.* **93** 073902
[14] Zhu Q Y, Fu Y Q, Hu D Q and Zhang Z M 2012 *Chin. Phys. B* **21** 064220
[15] Kurt H and Citrin D S 2007 *Opt. Express* **15** 1240
[16] Chien H T and Chen C C 2006 *Opt. Express* **14** 10759
[17] Roux F S and Leon D I 2006 *Phys. Rev. B* **74** 113103
[18] Wu Q, Gibbons J M and Park W 2008 *Opt. Express* **16** 941
[19] Kurt H, Colak E, Cakmak O, Caglayan H and Ozbay E 2008 *Appl. Phys. Lett.* **93** 171108
[20] Centeno E and Cassagne D 2005 *Opt. Lett.* **30** 2278
[21] Centeno E, Cassagne D and Albert J P 2006 *Phys. Rev. B* **73** 235119
[22] Akmansoy E, Centeno E, Vynck K, Cassagne D and Lourtioz J M 2008 *Appl. Phys. Lett.* **92** 133501
[23] Zhu Q Y, Fu Y Q, Zhang Z M, Xu Z J and Yu W X 2012 *Plasmonics* **7**
[24] Notomi M 2002 *Optical and Quantum Electronic* **34** 133